Published in final edited form as:
Cancer Res. 2014 August 15; 74(16): 4388–4397. doi:10.1158/0008-5472.CAN-14-1328.

Germline Mutation of *Bap1* Accelerates Development of Asbestos-Induced Malignant Mesothelioma

Jinfei Xu[1,5], **Yuwaraj Kadariya**[1,5], **Mitchell Cheung**[1], **Jianming Pei**[1], **Jacqueline Talarchek**[1], **Eleonora Sementino**[1], **Yinfei Tan**[1], **Craig W. Menges**[1], **Kathy Q. Cai**[2], **Samuel Litwin**[3], **Hongzhuang Peng**[4], **Jayashree Karar**[4], **Frank J. Rauscher**[4], and **Joseph R. Testa**[1]

[1]Cancer Biology Program, Fox Chase Cancer Center, Philadelphia, PA 19111

[2]Department of Pathology, Fox Chase Cancer Center, Philadelphia, PA 19111

[3]Biostatistics and Bioinformatics Facility, Fox Chase Cancer Center, Philadelphia, PA 19111

[4]Gene Expression and Regulation, Wistar Institute, Philadelphia, PA 32827

Abstract

Malignant mesotheliomas are highly aggressive tumors usually caused by exposure to asbestos. Germline inactivating mutations of *BAP1* predispose to mesothelioma and certain other cancers. However, why mesothelioma is the predominate malignancy in some BAP1 families and not others, and whether exposure to asbestos is required for development of mesothelioma in *BAP1* mutation carriers, are not known. To address these questions experimentally, we generated a $Bap1^{+/-}$ knockout mouse model to assess its susceptibility to mesothelioma upon chronic exposure to asbestos. $Bap1^{+/-}$ mice exhibited a significantly higher incidence of asbestos-induced mesothelioma than WT littermates(73% vs. 32%, respectively). Furthermore, mesotheliomas arose at an accelerated rate in $Bap1^{+/-}$ mice compared to WT animals(median survival, 43 weeks versus 55 weeks after initial exposure, respectively) and showed increased invasiveness and proliferation. No spontaneous mesotheliomas were seen in unexposed $Bap1^{+/-}$ mice followed for up to 87 weeks of age. Mesothelioma cells from $Bap1^{+/-}$ mice showed biallelic inactivation of *Bap1*, consistent with its proposed role as a recessive cancer susceptibility gene. Unlike in wild-type mice, mesotheliomas from $Bap1^{+/-}$ mice did not require homozygous loss of *Cdkn2a*. However, normal mesothelial cells and mesothelioma cells from $Bap1^{+/-}$ mice showed downregulation of

Corresponding Author: Joseph R. Testa, Cancer Biology Program, Fox Chase Cancer Center, 333 Cottman Avenue, Philadelphia, PA 19111. Phone: 215-728-2610; Fax: 215-214-1623; Joseph.Testa@fccc.edu.
[5]These authors contributed equally to this work.

Conflict of Interest: The authors have no potential conflicts of interest to disclose.

Authors' Contributions
Conception and design: J.R. Testa, F. Rauscher
Development of methodology: J. Xu, Y. Kadariya, M. Cheung, J. Pei, J. Talarchek, E. Sementino, Y. Tan, C.W. Menges, K. Cai, H. Peng, J. Karar
Acquisition of data (provided animals, provided facilities, etc.): J. Xu, Y. Kadariya, M. Cheung, J. Pei, J. Talarchek, E. Sementino, Y. Tan, C.W. Menges, K. Cai, H. Peng, J. Karar
Analysis and interpretation of data: J. Xu, Y. Kadariya, M. Cheung, J. Pei, J. Talarchek, E. Sementino, Y. Tan, C.W. Menges, K. Cai, S. Litwin, H. Peng, J. Karar, F. Rauscher, J.R. Testa
Writing, review, and/or revision of the manuscript: J.R. Testa, F. Rauscher, J. Xu, Y. Kadariya
Administrative, technical, or material support: Not applicable
Study supervision: J.R. Testa, F. Rauscher

Rb through a p16(Ink4a)-independent mechanism, suggesting that predisposition of *Bap1*$^{+/-}$ mice to mesothelioma may be facilitated, in part, by cooperation between Bap1 and Rb. Drawing parallels to human disease, these unbiased genetic findings indicate that *BAP1* mutation carriers are predisposed to the tumorigenic effects of asbestos and suggest that high penetrance of mesothelioma requires such environmental exposure.

Keywords

malignant mesothelioma; tumor suppressor genes; mouse tumor model; cancer predisposition; Rb; *Cdkn2a*

Introduction

Malignant mesothelioma (MM) is a highly aggressive, treatment-resistant cancer (1) causally related to asbestos exposure (2-4). Even three decades after peak commercial use of asbestos in the United States, about 3,200 MM cases are diagnosed here annually (5), and deaths due to MM are expected to increase by 5-10% per year in Europe over the next 25 years (4, 6). Moreover, a marked increase in MM is predicted in developing countries, where usage of asbestos is increasing exponentially(7).

Some individuals develop MM following exposure to small amounts of asbestos, while others exposed to heavy amounts do not(6), suggesting that genetic factors influence risk of this disease. In 1998, Jensen et al. identified a novel protein, BAP1 (BRCA1-associated protein 1), a nuclear-localized deubiquitylase, and intragenic homozygous rearrangements and deletions of *BAP1* were found in several lung carcinoma cell lines(8). More than a decade later, frequent somatic *BAP1* mutations were reported in metastatic uveal melanoma (UM), with one mutation observed in germline DNA(9).Shortly thereafter, recurring somatic mutations of *BAP1* were reported in MM(10-12). Indeed, the high incidence(~25-60%) of somatic *BAP1* mutations reported in MM implicates defects of this putative tumor suppressor gene along with frequent alterations of *CDKN2A*(13, 14), which encodes the tumor suppressors p16(INK4A) and p14(ARF), as well as *NF2*(15, 16) as the main drivers of MM tumorigenesis identified to date.

Importantly, in 2011 germline *BAP1* mutations were found in two families with multiple MMs (one also having two UMs) as well as in two sporadic cases affected by both MM and UM(11), the first demonstration that a hereditary defect can affect risk of MM. Concurrently, Wiesner et al. described germline *BAP1* mutations in two families with atypical melanocytic tumors, UM and cutaneous melanoma (CM)(17), and similar findings were reported by others (18). Collectively, the observations in these high-risk cancer families have led investigators to propose that germline *BAP1* mutations cause a novel cancer susceptibility syndrome characterized by a high incidence of MM, UM, CM and probably additional cancers(19, 20). The latter possibility is now certain, based on the subsequent identification of multiple BAP1 families with one or more renal cell carcinomas(21, 22).Other studies suggest that the clinical phenotype of the BAP1 syndrome may be expanded to other cancers such as lung adenocarcinoma, meningioma, breast carcinoma and paraganglioma(23-25).

We have hypothesized that when families with germline *BAP1* mutations are exposed to asbestos, MM may represent the predominant cancer observed(11). However, it is note worthy that members of neither of the MM families we reported had any obvious occupational exposure to asbestos, and only traces of asbestos were found in their homes. Similarly, Wiesner et al. (2012) reported a germline *BAP1* mutation in a European family with four MMs, none with any known exposure to asbestos(26). Thus, it is possible that exposure to carcinogenic mineral fibers may not be required for development of MM in *BAP1* mutation carriers. To test this hypothesis experimentally, mouse models would be invaluable. While conditional, whole-body (except brain) homozygous deletion of *Bap1* in adult mice recapitulates features of human myelodysplastic syndrome (MDS)(27), studies of germline heterozygous mutation of *Bap1* have not been described to date. We report here the generation of a $Bap1^{+/-}$ knockout mouse model used to assess predisposition to asbestos-induced MM. While no spontaneous MMs or MDS were seen in unexposed $Bap1^{+/-}$ mice followed for up to 20 months of age, such haploinsufficient mutant mice exhibited a markedly higher incidence and accelerated onset of asbestos-induced MM when compared to wild-type (WT) littermates. Mechanistically, we also demonstrate that predisposition of $Bap1^{+/-}$ mice to MM may be facilitated, in part, by cooperation between Bap1 and p16(Ink4a)-independent epigenetic inactivation of Rb.

Materials and Methods

Generation of *Bap1* knockout mice

Bap1 knockout mice in FVB genetic background were developed by zinc finger nuclease (ZFN) technology(28, 29), with the assistance of the Fox Chase Cancer Center (FCCC) Transgenic Mouse Facility, directed by Dietmar Kappes. Custom ZFNs targeting *Bap1* were designed and validated in mammalian cells by Sigma-Aldrich. Binding and cutting site of the ZFNs were TGCTCCCCAGTAGTCACTGATGGCTGTGCACG, with spacer between binding sites underlined. ZFN expression plasmids were linearized at the *Xba*I site located at the 3′ end of the *Fok*I ORF. 5′ capped and 3′ poly(A)-tailed message RNAs were prepared using MessageMAX™ T7 ARCA-Capped Message transcription (Cellscript) and poly(A) tailing kits (Epicentre Biotechnologies) and purified using an Ambion MEGAClear kit. The ZFN mRNAs were combined, microinjected into FVB blastocysts, which were implanted into pseudopregnant female mice. A schematic diagram showing the cutting site of the ZFNs and a portion of the *Bap1* knockout allele are depicted in Fig. 1A. Tails from resulting pups were genotypedby PCR amplification and sequencing to verify correct targeting (Fig. 1B). A *Bap1* knockout allele with deletion of exons 6 and 7 was identified which results in a frame shift and predicted premature truncation of the Bap1 protein. The net effect is similar to that observed in a human family having an intron 6 splice site mutation in *BAP1* that results in loss of exons 6 and 7 (11).

All mouse studies were performed according to NIH's *Guide for the Care and Use of Laboratory Animals*. The FCCC Committee on the Ethics of Animal Experiments approved the protocol for studies using asbestos.

Genotyping

Tail DNA samples were obtained through digestion and purification with a Gentra DNA extraction kit (Qiagen). The genotyping primers were as follows: forward, 5'-AGGCTTTGCTGCTAAATGAGA-3'; reverse, 5'-CCCTGAGACCCAGAAAATCA-3'. PCR cycling conditions were: 95°C (5 min), followed by 35 cycles at 95°C (30 sec), 58°C (30 sec), 72°C (45 sec), and 72°C (10 min). PCR products were resolved on gels and purified for DNA sequence analysis.

Asbestos injections

To assess susceptibility of *Bap1*$^{+/-}$ mice to the tumorigenic effects of asbestos, animals were injected intraperitoneally (i.p.)with UICC crocidolite (SPI Supplies) per our usual method(30-32). Representative examples of scanning electron microscopy (SEM) images of crocidolite fibers, and graphs illustrating fiber length distribution, are depicted in Supplemental Figure 1. Briefly, male *Bap1*$^{+/-}$ and WT littermate mice (25 per arm)at 8-10 weeks of age were injected i.p. with 800 μg/0.5 mL of crocidolite fibers in PBS every 21 days for a total of four injections (total, 3.2 mg/mouse). Mice were examined daily and sacrificed upon evidence of difficulty in breathing, severe weight loss, or when tumor burden was otherwise obvious. Upon detection of illness, mice were sacrificed by CO_2 asphyxiation, and internal organs were harvested and fixed in formalin for pathological analysis. When available, ascitic fluid was collected to generate tumor cell cultures.

Histopathology, immunohistochemistry and reverse transcriptase-PCR (RT-PCR)

Formalin-fixed/paraffin-embedded samples were cut into 5-μm sections and mounted onto positively charged microscope slides. Sections were dewaxed in xylene and hydrated through a graded ethanol series. Heat-induced antigen retrieval was performed in 10 mmol/L sodium citrate (pH6.0) in a microwave for 10 min, followed by blocking of endogenous peroxidase activity by immersion of slides in 3% H_2O_2 in PBS for 30 min. To confirm the diagnosis of MM, immunohistochemistry (IHC) was performed for various markers of MM, including calretinin, cytokeratin 18/19, vimentin and WT1 using antibodies from Sigma and a mesothelin antibody from Santa Cruz. Following incubation of slides with the designated antibodies, detection was with biotinylated secondary antibodies. Sections were stained with DAB and counterstained with hematoxylin. To assess cell proliferation and apoptosis, IHC staining of tumors was performed with antibodies for Ki-67 (Dako)and cleaved caspase 3(Cell Signaling), respectively. Tumors were also stained with a BAP1 antibody from Santa Cruz to evaluate the presence and localization of Bap1.

In MMs with limited tissue available for IHC, RT-PCR analysis of tumor tissue and/or primary cell cultures was occasionally used. Mice were scored as having MM if tumor cells exhibited a combination of three or more MM markers, including mesothelin, E-cadherin, N-cadherin, and cytokeratin 18/19 as assessed by RT-PCR(30). Control *Gapdh* was used to assess template integrity.

Hematological assessment of *Bap1*$^{+/-}$ mice

In several *Bap1*$^{+/-}$ mice not exposed to asbestos, hematological assessment was performed on bone marrow and peripheral blood to rule out the possibility of MDS, a phenotype observed in *Bap1* conditional knockout mice (27), or other hematological disease. After sacrificing mice, bone marrow aspirates were obtained from femurs. Blood was collected for complete blood counts and cytological evaluation.

Primary tumor and normal mesothelial cell cultures

Primary MM cells were isolated from ascitic fluid and/or peritoneal lavage from *Bap1*$^{+/-}$ and WT mice as described (30). Cells were cultured and maintained in Dulbecco's modified Eagle medium (DMEM) containing 10% FBS, 2 mmol/L L-glutamine, and penicillin (50 units/mL)/streptomycin (50 μg/mL). Cell cultures used for molecular analyses were from passages ≤10. PCR analysis was carried out to confirm expression of mesothelial markers.

Primary mesothelial cells were obtained from 6- to 8-week-old *Bap1*$^{+/-}$ and WT mice that were not exposed to asbestos, according to the method of Bot et al.(33). Mesothelial cell cultures used for molecular analyses were from passages ≤3.

Immunoblotting

Immunoblots were prepared with 50 μg of protein/sample, as described (31). Primary antibodies against Bap1 (Bethyl, 1:1000 dilution), Rb (BD Biosciences, 1:1000 dilution), and β-actin (Santa Cruz, 1:1000 dilution) were used. Appropriate secondary antibodies (anti-rabbit-, anti-mouse- and anti-goat-HRP – Santa Cruz) were used at a 1:2,000 dilution.

Array-based comparative genomic hybridization analysis

Array-CGH (aCGH) with Agilent 244K genomic DNA arrays was performed on asbestos-induced MMs from *Bap1*$^{+/-}$ and WT mice as previously described (31). Briefly, genomic DNA was isolated, restriction enzyme digested, fluorescently labeled, purified, and hybridized to Agilent arrays. After scanning of chips on an Agilent scanner, data were extracted using Feature Extraction Software, and output was imported into CGH Analytics for DNA Copy Number Analysis (Agilent).

Cell viability assay

MM cells were seeded onto 96-well plates at a density of 2,000 cells/well. Cells were immediately treated with 20 μM HLM006474, 5 μM LY2835219,or DMSO vehicle for 72 h. MTS reagent was added, and absorbance was determined at 490 nm as a read out of cell viability.

Immunoprecipitation (IP) and Ub-AMC assay

Whole cell lysates were extracted with NP40 lysis buffer. Bap1 antibody was pre-coated on protein A/G PLUS-Agarose (Santa Cruz) in binding buffer (50 mM Tris-HCl, pH 7.4, 150 mM NaCl, 2 mM EDTA, 0.25% NP40, 2% BSA) at 4°C overnight. Five mg of each whole cell lysate was used for IP with pre-coated anti-Bap1 agarose beads in 2 ml reaction volume at 4°C for 2 h. IP complex resins were washed with buffer three times, with final wash done

in 1x ubiquitin 7-amido-4-methylcoumarin (Ub-AMC) assay reaction buffer. The Ub-AMC activity reaction was performed with IP complex resin in 1x Ub-AMC assay reaction buffer (20 mM HEPES, pH 7.5, 100 mM NaCl, 1 mM EDTA, 5 mM DTT, and 0.05% [w/v] Tween-20) and 10 nM Ub-AMC (total volume, 50 μl) and incubated at 25°C for 15 min. The resin was spun down, and 25 μl of supernatant was used for the Ub-AMC assay. Fluorescence was measured at excitation and emission wavelengths of 355 nm and 460 nm, respectively, with hydrolysis rate corrected for background signal (no enzyme).

5-Aza-2'-deoxycytidine (5-Aza-CdR)treatment and methylated DNA immunoprecipitation (MeDIP) assay

To assess epigenetic modification of the *Rb1* gene in MM cells, initially total Rb expression was evaluated by treatment of cells with 10 μM and 20 μM of5-Aza-CdRfor 72 h. MeDIP was carried out according to the manufacturer's protocol(Active Motif). For each sample, a 1 μl aliquot was used for PCR analysis of the *Rb1* promoter, and nested PCR was carried out. Primers used in the first PCR were as follows. Forward: 5'-CCTTGTCTCCAGAAGGCCAC-3', reverse: 5'-TACAAAAATAATGGGAACGTCCCC-3' at 95°C for 5 min followed by 45 cycles at 95°C (30 sec), 60°C (30 sec), 72°C (45 sec), and72°C (10 min). Primers used in the second PCR were as follows. Forward: 5'-ACGACGCGGGCGGAGAC-3', reverse: 5'-TCAGTGGGGAACCGGGG-3' at 95°C (5 min) followed by 45 cycles of 95°C (30 sec), 60°C (30 sec), and 72°C (30 sec), and 72°C (10 min).

Results

Phenotype of *Bap1* knockout mice

To assess spontaneous tumor formation, 27 $Bap1^{+/-}$ and 30 WT mice were followed long term. As reported previously (27),homozygous loss of *Bap1* was found to be lethal in early embryogenesis(post conception day 7.5-8.5), whereas heterozygous $Bap1^{+/-}$ mice (genotyping shown in Fig. 1B)are viable with no obvious anatomical abnormalities. To date, only one spontaneous tumor, a squamous cell carcinoma (SCC) of mammary origin, has been detected in our $Bap1^{+/-}$ mice, although most of the remaining untreated animals are still only 11 to 20months of age. Peripheral blood smears and CBC of four 3-month-old $Bap1^{+/-}$ mice and three18-month-old $Bap1^{+/-}$ mice(including the mouse with the SCC) were comparable to that observed in WT littermates. Bone marrow smears from the three 18-month-old $Bap1^{+/-}$ mice showed no evidence of MDS or other hematological disease, and no macroscopic and microscopic abnormalities of the uvea, skin, mesothelial tissues, or other organs were observed except for the single SCC. To date, one tumor, a thymic lymphoma, has been observed in WT littermates.

$Bap1^{+/-}$ mice are predisposed to development of asbestos-induced MMs

$Bap1^{+/-}$ mice and WT littermates were chronically injected i.p. with crocidolite asbestos fibers starting at 8–10 weeks of age. Animals were monitored continuously over 16 months. Abdominal swelling was observed in $Bap1^{+/-}$ mice as early as 20 weeks after the first injection of asbestos, whereas WT animals did not begin showing this effect until 27 weeks after the initial injection. Eventually, 90% of the asbestos-exposed $Bap1^{+/-}$ mice showed

abdominal distention, and ~60% of these were found to have as cites when sacrificed. A few others had abdominal swelling due to intestinal distention. Almost all of these mice showed liver abnormalities, pancreatic fibrosis, intestinal adhesions, and thickenings of the peritoneum, mesentery and diaphragm. The *Bap1*$^{+/-}$ mice were found to succumb to disease earlier than their WT littermates, with a median survival of 43 weeks from the time of the first asbestos injection in *Bap1*$^{+/-}$ mice versus 55 weeks in WT mice (Fig. 1C) (Wilcox on 2-sample test, $p < 0.0001$). Deaths due to peritoneal MM occurred in 73% of *Bap1*$^{+/-}$ mice that could be pathologically evaluated compared to only 32% of WT animals(Fisher's exact test, $p < 0.01$). Other deaths in WT and *Bap1*$^{+/-}$ mice occurred mainly due to plaque-related organ failure or intestinal obstructions related to fibrosis. It is also noteworthy that while all asbestos-exposed *Bap1*$^{+/-}$ mice succumbed from MM and other asbestos-related disease by 57 weeks, 5 (20%) of WT mice were still alive and asymptomatic at this time, 69 weeks after initial exposure to asbestos.

Asbestos-induced MMs in *Bap1*$^{+/-}$ mice show increased aggressiveness

Examples of the histopathology of asbestos-induced MMs from WT and *Bap1* knockout mice are shown in Supplemental Figure 2. Notably, asbestos-induced MMs seen in *Bap1*$^{+/-}$ mice were consistently larger and more aggressive than those found in WT littermates, often with invasion to the pancreas, liver, and/or intestinal smooth muscle (Suppl. Fig. 3); occasional metastasis to the lungs was also observed in the *Bap1*$^{+/-}$ mice. Moreover, tumors in *Bap1*$^{+/-}$ mice were more proliferative based on Ki-67 staining (Suppl. Fig. 2). Immunohistochemical staining of tumors from both WT and *Bap1*$^{+/-}$ mice revealed strong staining for markers of MM, such as mesothelin (Suppl. Fig. 4). Importantly, Bap1 staining was observed in MMs from WT mice but was absent in MMs from *Bap1*$^{+/-}$ mice (Suppl. Fig. 4).

MM cells from *Bap1*$^{+/-}$ mice show biallelic inactivation of *Bap1* and *Cdkn2a*-independent downregulation of Rb

We were able to generate primary MM cell cultures from as cites or peritoneal lavage of several *Bap1*$^{+/-}$ and WT mice, and multiple analyses were performed on early passage cells, as summarized below. Verification of the mesothelial origin of the cells was performed by semi-quantitative RT-PCR using primers against three MM markers: mesothelin, N-cadherin, and cytokeratin 18 (Fig. 2A). We also performed semi-quantitative RT-PCR using primers against *Bap1*. All three MM cultures derived from asbestos-exposed WT mice showed abundant expression of wild-type *Bap1* mRNA, whereas MM cells from *Bap1*$^{+/-}$ mice lacked expression of wild-type *Bap1* but did retain expression of a truncated form of *Bap1* mRNA (Fig. 2A). Sequence analysis of the RT-PCR products confirmed that the truncated *Bap1* mRNA did not contain exons 6 and 7, consistent with its derivation from the germline mutant *Bap1* allele. Western blot analysis demonstrated abundant expression of Bap1 protein in MMs from WT mice but loss of Bap1 expression in MMs from *Bap1*$^{+/-}$ mice (see below). To ascertain why the tumor cells from the *Bap1*$^{+/-}$ mice did not show Bap1 protein expression, we designed PCR primers encompassing the *Bap1* knockout site to assess whether there was loss of the WT *Bap1* allele. PCR analyses on genomic DNA isolated from cells lacking Bap1 protein expression demonstrated that the WT allele of *Bap1* was absent (Fig. 2B), consistent with loss of heterozygosity. Additionally, assessment by

Ub-AMC assay revealed Bap1 deubiquitinating enzyme activity in MM cells from WT mice but not in MM cells from *Bap1*$^{+/-}$ mice(Fig. 2C).

Intriguingly, aCGH analysis revealed that all three MM cell cultures derived from WT mice had homozygous deletions of the *Cdkn2a/Cdkn2b* loci, whereas MM cells from two *Bap1*$^{+/-}$ mice did not (Fig. 3A). Semi-quantitative RT-PCR analyses confirmed that expression of *Cdkn2a*(*p16Ink4a* and *p19Arf*) and *Cdkn2b* (*p15Ink4b*)was absent in tumor cells from WT mice but present in cells from *Bap1*$^{+/-}$ mice (Fig. 2A). This result prompted us to examine the expression and phosphorylation status of the Rb tumor suppressor, since inactivation of Rb by hyperphosphorylation is the major downstream effect resulting from *p16Ink4a* loss. Interestingly, expression of Rb was strikingly decreased in MM cells from *Bap1*$^{+/-}$ mice, which showed no expression of Bap1 protein, when compared toBap1-expressing MM cells from WT tumors that lacked expression of *p16Ink4a*(Fig. 3B). To determine the reason why Rb phosphorylation was drastically reduced, we first assessed the expression of total Rb protein. Surprisingly, expression of total Rb protein was markedly decreased in tumor cells from *Bap1*$^{+/-}$ mice. Quantitative RT-PCR revealed that the mRNA expression levels of *Rb1* in MM cells from the *Bap1*$^{+/-}$ mice were less than half that of tumor cells from WT mice (Fig. 3B). Intriguingly, expression of *Rb1* mRNA and Rb protein was also found to be down regulated in early passage (≤3) normal mesothelial cells isolated from *Bap1*$^{+/-}$ mice compared to those from WT mice (Fig. 3C), suggesting that reduced expression of Rb may contribute to the enhanced susceptibility to the carcinogenic effects of asbestos observed in *Bap1*$^{+/-}$ mice.

Aberrant expression of Rb in MM cells from *Bap1*$^{+/-}$ mice occurs by epigenetic regulation

Since aCGH analysis did not uncover any DNA copy number changes at the*Rb1* locus in any of the MM cell cultures tested, we hypothesized that the decreased *Rb1* expression was due to aberrant epigenetic modification of the *Rb1* gene in MM cells from *Bap1*$^{+/-}$ mice. In addition, *BAP1* mutation and decreased *BAP1* expression have been shown to be associated with increased methylation of PRC2 target genes(34), and GC-rich DNA can itself suffice to recruit PRC2 even in the absence of more complex DNA sequence motifs(35). An analysis of the *Rb1* promoter sequence found in GenBank revealed a promoter CpG island containing 101 CpG and GpC dinucleotides within 300 bp upstream or downstream of the transcription initiation site of the *Rb1* gene. Thus, reduced expression of Rb protein in tumor cells from *Bap1*$^{+/-}$ mice could be due to inactivation of PRC2 resulting from loss of the Bap1 protein. Indeed, we found that treatment of *Bap1*-null MM cells with 5-Aza-CdRsignificantly increased the expression of Rb (Fig. 4A). Moreover, analysis by MeDIP assay revealed that methylation modifications of the *Rb1* promoter were markedly elevated in *Bap1*-null MM cells compared to MM cells from WT mice(Fig. 4B). Collectively, these findings suggest that the lower expression of *Rb1 in Bap1*-null MM cells is due to hypermethylation of the*Rb1* promoter.

To test whether Rb inactivation contributes to the malignant phenotype of MM cells from *Bap1*$^{+/-}$ mice, the cells were treated with either an E2f inhibitor or a Cdk4/6 dual inhibitor (Fig. 4C). Interestingly, we found MM cell cultures from both WT and *Bap1*$^{+/-}$ mice were sensitive to the E2f inhibitor, but only the cells derived from WT mice were highly sensitive

to the Cdk4/6 inhibitor. p16(Ink4a)is known to inhibit the activity of a complex composed by cyclin D, Cdk4 and Cdk6, leading to inactivation of Rb by phosphorylation, thereby abolishing binding between Rb and E2f, leading to activation of E2f target genes. Thus, an inhibitor of Cdk4/6 would be expected to block the inhibition of Rb, resulting in enhanced binding of Rb to E2f and to decreased cell proliferation by diminishing the transcriptional activity of E2f in cells lacking expression of p16(Ink4a). Indeed, we found that WT tumor cells lacking expression of p16(Ink4a), but retaining expression of Bap1, were much more sensitive to a Cdk4/6 inhibitor than *Bap1*-null cells that retained expression of p16(Ink4a) (Fig. 4C). These results suggest that *Bap1*-deficient MM cells are still dependent on E2f activation, but through a mechanism independent of *p16(Ink4a)* loss.

Discussion

Although we have seen evidence of only a single spontaneous tumor in *Bap1*$^{+/-}$ mice to date, our mice are still ≤20 months of age at this time. Thus, we cannot rule out the possibility that spontaneous MMs and various other tumors will arise as our mice age further. Germane to this, mice with heterozygous germline inactivation of *Nf2*, another tumor suppressor gene commonly mutated in MM, developed a variety of spontaneous malignant tumors late in life (10-30 months of age); most animals died of osteosarcomas, with a median survival of 19 months in females and23 months in males(36). Continued study of our cohort of untreated *Bap1*$^{+/-}$ mice will permit us to determine if older mice are predisposed to a particular spectrum of solid tumors or hematopoietic diseases, possibly including MM or MDS, the latter reported in homozygous conditional *Bap1* knockout mice(27).

Upon exposure to asbestos fibers, we found a high penetrance of MM in *Bap1*$^{+/-}$ mice when compared to WT littermates. Importantly, MM development was significantly accelerated and more aggressive in the *Bap1*$^{+/-}$ mice, providing unbiased genetic evidence supporting a fundamental role of *Bap1* loss in MM pathogenesis. The accelerated rate of death due to asbestos-related disease in *Bap1*$^{+/-}$ mice compared to WT mice (median survival 43 weeks vs. 55 weeks in WT mice, respectively) is similar to the accelerated onset and shorter median survivals that we observed previously in mice with haploinsufficiency for other tumor suppressor genes – *Cdkn2a/p16(Ink4a)*, *Cdkn2a/p19Arf*, and *Nf2* – that are thought to act as key drivers in MM pathogenesis(30, 31, 37). Moreover, like the MMs from these other mutant mouse models, MMs from *Bap1*$^{+/-}$ mice showed biallelic inactivation of the predisposing gene, indicating that *Bap1* acts as a bona fide tumor suppressor gene in MM pathogenesis. Thus, the experimental data presented here are consistent with the notion that *Bap1* inactivation plays an important role in MM development.

With regard to tumor histology, it is noteworthy that all of the MMs in our *Bap1*$^{+/-}$ and WT mice appeared to be biphasic, whereas sarcomatoid MMs were predominant in our earlier studies of *Cdkn2a/p16(Ink4a)*$^{+/-}$ and *Cdkn2a/p19(Arf)*$^{+/-}$ mice (37). In our report of human *BAP1* families(11), all of the available MM specimens seen in *BAP1* mutation carriers were of the epithelial type, although the significance of this finding could not be established due to the relatively small number of cases evaluated. In sporadic MM, several groups have reported that somatic mutations of *BAP1* occur primarily in epithelioid tumors (11, 12, 38),

whereas Zauderer et al. could find no obvious difference in tumor histology among MMs with and without somatic *BAP1* mutations (39).

Collectively, the experimental findings summarized here indicate that germline *Bap1* mutation predisposes to the tumorigenic effects of asbestos. By using an unbiased genetic model system and chronic exposure to asbestos, we have been able to demonstrate that germline haploinsufficiency for *Bap1* causes increased susceptibility to asbestos-induced MM formation, which may be facilitated, at least in part, by a p16(Ink4a)-independent mechanism involving epigenetic dysregulation of Rb. Although loss of p16(INK4A) expression, via homozygous deletion of *CDKN2A*, has long been known to be a frequent finding in human MM(13, 14), a recent integrated genomic analysis of 53 sporadic pleural MMs revealed that 6 of 12 tumors with *BAP1* mutations did not exhibit allelic losses of *CDKN2A*; moreover, 17 of 20 tumors with homozygous losses of *CDKN2A* did not show point mutations in *BAP1*(10). It is also noteworthy that our earlier aCGH analysis of MMs from two unrelated *BAP1* mutation carriers revealed no homozygous losses of *CDKN2A*, although one of the tumors did exhibit monosomy 9, resulting in heterozygous loss of *CDKN2A*(11). Thus, our findings in an experimental model system, together with these clinical findings, indicate that *BAP1* inactivation in MM may not require homozygous loss of *CDKN2A/p16(INK4A)*. Importantly, however, our data suggest that dysregulation of the Rb path way may be required for *Bap1*-driven MM pathogenesis, at least in an experimental model. The fact that expression of Rb is diminished in both normal mesothelial cells and MM cells from $Bap1^{+/-}$ mice suggests that Rb loss may contribute mechanistically to accelerated MM onset and increased proliferation of tumor cells observed in $Bap1^{+/-}$ mice. Relevant to this possibility, germline heterozygous mutations of other cancer susceptibility genes, such as the tumor suppressor gene *VHL* connected with hereditary renal cancer, have been shown to alter the mRNA expression profiles of primary cultures of phenotypically normal epithelial cells in a gene-specific manner, and in some instances the expression data confirmed what is known about key tumorigenic pathways affected by biallelic mutations of such tumor suppressor genes (40). In $Bap1^{+/-}$ mice, heterozygous (“one hit”) mutation is associated with alteration in the expression of a central node (Rb) in a cellular corridor – the p16(Ink4a)-Rb pathway – that is strongly implicated in MM pathogenesis generally. Whether this novel finding translates to its human counterpart will be the subject of future investigation.

Our findings in our $Bap1^{+/-}$ mouse model suggest that early onset and high penetrance of MM may require exposure to carcinogenic mineral fibers. Germane to this possibility, the initial two reports of families with germline *BAP1* mutations were paradoxical, with our group reporting two families with multiple (5 and 7) MMs(11), and a second group describing two families with atypical melanocytic neoplasms but no MMs (17), although a follow up study uncovered a single MM in one of the latter families(26). Rather than representing two dissimilar cancer-related syndromes, it became apparent that germline *BAP1* mutations are associated with a spectrum of neoplasms, suggesting that BAP1 has acritical tumor suppressor function in a variety of tissues (41, 42). The first reports of BAP1 families(17, 26) involved a selection bias, in the sense that the investigators were drawn to their families because of the high incidence of a particular cancer type, but subsequent work

has revealed that MM and atypical melanocytic neoplasms are not always the predominant tumor types observed in BAP1 families (19, 23). Thus, as originally proposed, MM may only predominate when there is exposure to asbestos(11). Based on our earlier work on two BAP1 families with multiple MMs(11),it appears that the level of asbestos exposure need not be high in *BAP1* mutation carriers, as occupational histories on those families did not suggest any obvious exposure, and only modest or trace levels of asbestos were found in their homes. In the *in vivo* tumorigenicity studies reported here, the level of asbestos exposure used was sufficient to induce deaths in all mice with germline haploinsufficiency for *Bap1* but not in all WT animals. Drawing parallels to humans, our findings provide experimental support for the idea that *BAP1* mutation carriers may be highly susceptible to MM even at modest levels of asbestos exposure that would be considerably less tumorigenic in the general population and, thus, would require close clinical monitoring with the goal of early detection and intervention.

Supplementary Material

Refer to Web version on PubMed Central for supplementary material.

Acknowledgments

The authors thank Yu Cao (FCCC) for technical assistance with aCGH hybridizations and Jamie Ford (University of Pennsylvania Nanoscale Characterization Facility)for SEM analysis of asbestos samples. The following FCCC core services assisted this project: Laboratory Animal, Transgenic Mouse, Genomics, Cell Culture, DNA Sequencing, Cell Sorting, Histopathology, and Biostatistics and Bioinformatics Facilities.

Grant Support

Work supported by NCI grants CA175691 (J.R. Testa and F.J. Rauscher) and CA-06927 (J.R. Testa and S. Litwin), a grant from the Mesothelioma Applied Research Foundation (M. Cheung and J.R. Testa), an appropriation from the Commonwealth of Pennsylvania, and a gift from the Local #14 Mesothelioma Fund of the International Association of Heat and Frost Insulators & Allied Workers.

References

1. Flores RM, Pass HI, Seshan VE, Dycoco J, Zakowski M, Carbone M, et al. Extrapleural pneumonectomy versus pleurectomy/decortication in the surgical management of malignant pleural mesothelioma: results in 663 patients. J Thorac Cardiovasc Surg. 2008; 135:620–626. [PubMed: 18329481]
2. Wagner JC, Sleggs CA, Marchand P. Diffuse pleural mesothelioma and asbestos exposure in the North Western Cape Province. Br J Ind Med. 1960; 17:260–271. [PubMed: 13782506]
3. Kamp DW. Asbestos-induced lung diseases: an update. Transl Res. 2009; 153:143–152. [PubMed: 19304273]
4. Moolgavkar SH, Meza R, Turim J. Pleural and peritoneal mesotheliomas in SEER: age effects and temporal trends, 1973 – 2005. Cancer Causes Control. 2009; 20:935–44. [PubMed: 19294523]
5. Henley SJ, Larson TC, Wu M, Antao VC, Lewis M, Pinheiro GA, et al. Mesothelioma incidence in 50 states and the District of Columbia, United States, 2003 – 2008. Int J Occup Environ Health. 2013; 19:1–10. [PubMed: 23582609]
6. Carbone M, Ly BH, Dodson RF, Pagano I, Morris PT, Dogan UA, et al. Malignant mesothelioma: facts, myths, and hypotheses. J Cell Physiol. 2012; 227:44–58. [PubMed: 21412769]
7. Burki T. Health experts concerned over India's asbestos industry. Lancet. 2010; 375:626–627. [PubMed: 20198723]

8. Jensen DE, Proctor M, Marquis ST, Gardner HP, Ha SI, Chodosh LA, et al. BAP1: a novel ubiquitin hydrolase which binds to the BRCA1 RING finger and enhances BRCA1-mediated cell growth suppression. Oncogene. 1998; 16:1097–1112. [PubMed: 9528852]
9. Harbour JW, Onken MD, Roberson ED, Duan S, Cao L, Worley LA, et al. Frequent mutation of BAP1 in metastasizing uveal melanomas. Science. 2010; 330:1410–1413. [PubMed: 21051595]
10. Bott M, Brevet M, Taylor BS, Shimizu S, Ito T, Wang L, et al. The nuclear deubiquitinase BAP1 is commonly inactivated by somatic mutations and 3p21.1 losses in malignant pleural mesothelioma. Nat Genet. 2011; 43:668–672. [PubMed: 21642991]
11. Testa JR, Cheung M, Pei J, Below JE, Tan Y, Sementino E, et al. Germline BAP1 mutations predispose to malignant mesothelioma. Nat Genet. 2011; 43:1022–1025. [PubMed: 21874000]
12. Yoshikawa Y, Sato A, Tsujimura T, Emi M, Morinaga T, Fukuoka K, et al. Frequent inactivation of the BAP1 gene in epithelioid-type malignant mesothelioma. Cancer Sci. 2012; 103:868–874. [PubMed: 22321046]
13. Cheng JQ, Jhanwar SC, Klein WM, Bell DW, Lee W-C, Altomare DA, et al. *p16* alterations and deletion mapping of 9p21-p22 in malignant mesothelioma. Cancer Res. 1994; 54:5547–5551. [PubMed: 7923195]
14. Xiao S, Li D, Vijg J, Sugarbaker DJ, Corson JM, Fletcher JA. Codeletion of p15 and p16 in primary malignant mesothelioma. Oncogene. 1995; 11:511–515. [PubMed: 7630635]
15. Bianchi AB, Mitsunaga S-I, Cheng JQ, Klein WM, Jhanwar SC, Seizinger B, et al. High frequency of inactivating mutations in the neurofibromatosis type 2 gene (*NF2*) in primary malignant mesotheliomas. Proc Natl Acad Sci U S A. 1995; 92:10854–10855. [PubMed: 7479897]
16. Sekido Y, Pass HI, Bader S, Mew DJY, Christman MF, Gazdar AF, et al. Neurofibromatosis type 2 (*NF2*) gene is somatically mutated in mesothelioma but not in lung cancer. Cancer Res. 1995; 55:1227–1231. [PubMed: 7882313]
17. Wiesner T, Obenauf AC, Murali R, Fried I, Griewank KG, Ulz P, et al. Germline mutations in BAP1 predispose to melanocytic tumors. Nat Genet. 2011; 43:1018–1021. [PubMed: 21874003]
18. Njauw CN, Kim I, Piris A, Gabree M, Taylor M, Lane AM, et al. Germline BAP1 inactivation is preferentially associated with metastatic ocular melanoma and cutaneous-ocular melanoma families. PLoS One. 2012; 7:e35295. [PubMed: 22545102]
19. Carbone M, Yang H, Pass HI, Krausz T, Testa JR, Gaudino G. BAP1 and cancer. Nat Rev Cancer. 2013; 13:153–159. [PubMed: 23550303]
20. Testa JR, Malkin D, Schiffman JD. Connecting molecular pathways to hereditary cancer risk syndromes. Am Soc Clin Oncol Educ Book. 2013:81–90. [PubMed: 23714463]
21. Popova T, Hebert L, Jacquemin V, Gad S, Caux-Moncoutier V, Dubois-d'Enghien C, et al. Germline BAP1 mutations predispose to renal cell carcinomas. Am J Hum Genet. 2013; 92:974–980. [PubMed: 23684012]
22. Farley MN, Schmidt LS, Mester JL, Pena-Llopis S, Pavia-Jimenez A, Christie A, et al. A novel germline mutation in BAP1 predisposes to familial clear-cell renal cell carcinoma. Mol Cancer Res. 2013; 11:1061–1071. [PubMed: 23709298]
23. Abdel-Rahman MH, Pilarski R, Cebulla CM, Massengill JB, Christopher BN, Boru G, et al. Germline BAP1 mutation predisposes to uveal melanoma, lung adenocarcinoma, meningioma, and other cancers. J Med Genet. 2011; 48:856–859. [PubMed: 21941004]
24. Wadt K, Choi J, Chung JY, Kiilgaard J, Heegaard S, Drzewiecki KT, et al. A cryptic BAP1 splice mutation in a family with uveal and cutaneous melanoma, and paraganglioma. Pigment cell & melanoma research. 2012; 25:815–818. [PubMed: 22889334]
25. Pilarski R, Cebulla CM, Massengill JB, Rai K, Rich T, Strong L, et al. Expanding the clinical phenotype of hereditary BAP1 cancer predisposition syndrome, reporting three new cases. Genes Chromosomes Cancer. 2014; 53:177–182. [PubMed: 24243779]
26. Wiesner T, Fried I, Ulz P, Stacher E, Popper H, Murali R, et al. Toward an improved definition of the tumor spectrum associated with BAP1 germline mutations. J Clin Oncol. 2012; 30:e337–e340. [PubMed: 23032617]
27. Dey A, Seshasayee D, Noubade R, French DM, Liu J, Chaurushiya MS, et al. Loss of the tumor suppressor BAP1 causes myeloid transformation. Science. 2012; 337:1541–1546. [PubMed: 22878500]

28. Meyer M, de Angelis MH, Wurst W, Kühn R. Gene targeting by homologous recombination in mouse zygotes mediated by zinc-finger nucleases. Proc Natl Acad Sci US A. 2010; 107:15022–15026.
29. Cui X, Ji D, Fisher DA, Wu Y, Briner DM, Weinstein EJ. Targeted integration in rat and mouse embryos with zinc-finger nucleases. Nat Biotechnol. 2011; 29:64–67. [PubMed: 21151125]
30. Altomare DA, Vaslet CA, Skele KL, De Rienzo A, Devarajan K, Jhanwar SC, et al. A mouse model recapitulating molecular features of human mesothelioma. Cancer Res. 2005; 65:8090–8095. [PubMed: 16166281]
31. Altomare DA, Menges CW, Pei J, Zhang L, Skele-Stump KL, Carbone M, et al. Activated TNF-alpha/NF-kappaB signaling via down-regulation of Fas-associated factor 1 in asbestos-induced mesotheliomas from Arf knockout mice. Proc Natl Acad Sci U S A . 2009; 106:3430–3435.
32. Menges CW, Kadariya Y, Altomare D, Talarchek J, Neumann-Domer E, Wu Y, et al. Tumor suppressor alterations cooperate to drive aggressive mesotheliomas with enriched cancer stem cells via a p53-miR34a-c-Met axis. Cancer Res. 2014; 74:1261–1271. [PubMed: 24371224]
33. Bot J, Whitaker D, Vivian J, Lake R, Yao V, McCauley R. Culturing mouse peritoneal mesothelial cells. Pathol Res Pract. 2003; 199:341–344. [PubMed: 12908525]
34. Sato T, Kaneda A, Tsuji S, Isagawa T, Yamamoto S, Fujita T, et al. PRC2 overexpression and PRC2-target gene repression relating to poorer prognosis in small cell lung cancer. SciRep. 2013; 3:1911.
35. Mendenhall EM, Koche RP, Truong T, Zhou VW, Issac B, Chi AS, et al. GC-rich sequence elements recruit PRC2 in mammalian ES cells. PLoS Genet. 2010; 6:e1001244. [PubMed: 21170310]
36. McClatchey AI, Saotome I, Mercer K, Crowley D, Gusella JF, Bronson RT, et al. Mice heterozygous for a mutation at the *Nf2* tumor suppressor locus develop a range of highly metastatic tumors. Genes Dev. 1998; 12:1121–1133. [PubMed: 9553042]
37. Altomare DA, Menges CW, Xu J, Pei J, Zhang L, Tadevosyan A, et al. Losses of both products of the Cdkn2a/Arf locus contribute to asbestos-induced mesothelioma development and cooperate to accelerate tumorigenesis. PLoS One. 2011; 6:e18828. [PubMed: 21526190]
38. de Reyniès A, Jaurand MC, Renier A, Couchy GIH, Elarouci N, et al. Molecular classification of malignant pleural mesothelioma: identification of a poor prognosis subgroup linked to the epithelial-to-mesenchymal transition. Clin Cancer Res. 2014; 20:1323–1334. [PubMed: 24443521]
39. Zauderer MG, Bott M, McMillan R, Sima CS, Rusch V, Krug LM, et al. Clinical characteristics of patients with malignant pleural mesothelioma harboring somatic BAP1 mutations. J Thorac Oncol. 2013; 8:1430–1433. [PubMed: 24128712]
40. Stoyanova R, Clapper ML, Bellacosa A, Henske EP, Testa JR, Ross EA, et al. Altered gene expression in phenotypically normal renal cells from carriers of tumor suppressor gene mutations. Cancer BiolTher. 2004; 3:1313–1321.
41. Goldstein AM. Germline BAP1 mutations and tumor susceptibility. Nat Genet. 2011; 43:925–926. [PubMed: 21956388]
42. Cheung M, Talarchek J, Schindeler K, Saraiva E, Penney LS, Ludman M, et al. Further evidence for germline BAP1 mutations predisposing to melanoma and malignant mesothelioma. Cancer Genet. 2013; 206:206–210. [PubMed: 23849051]

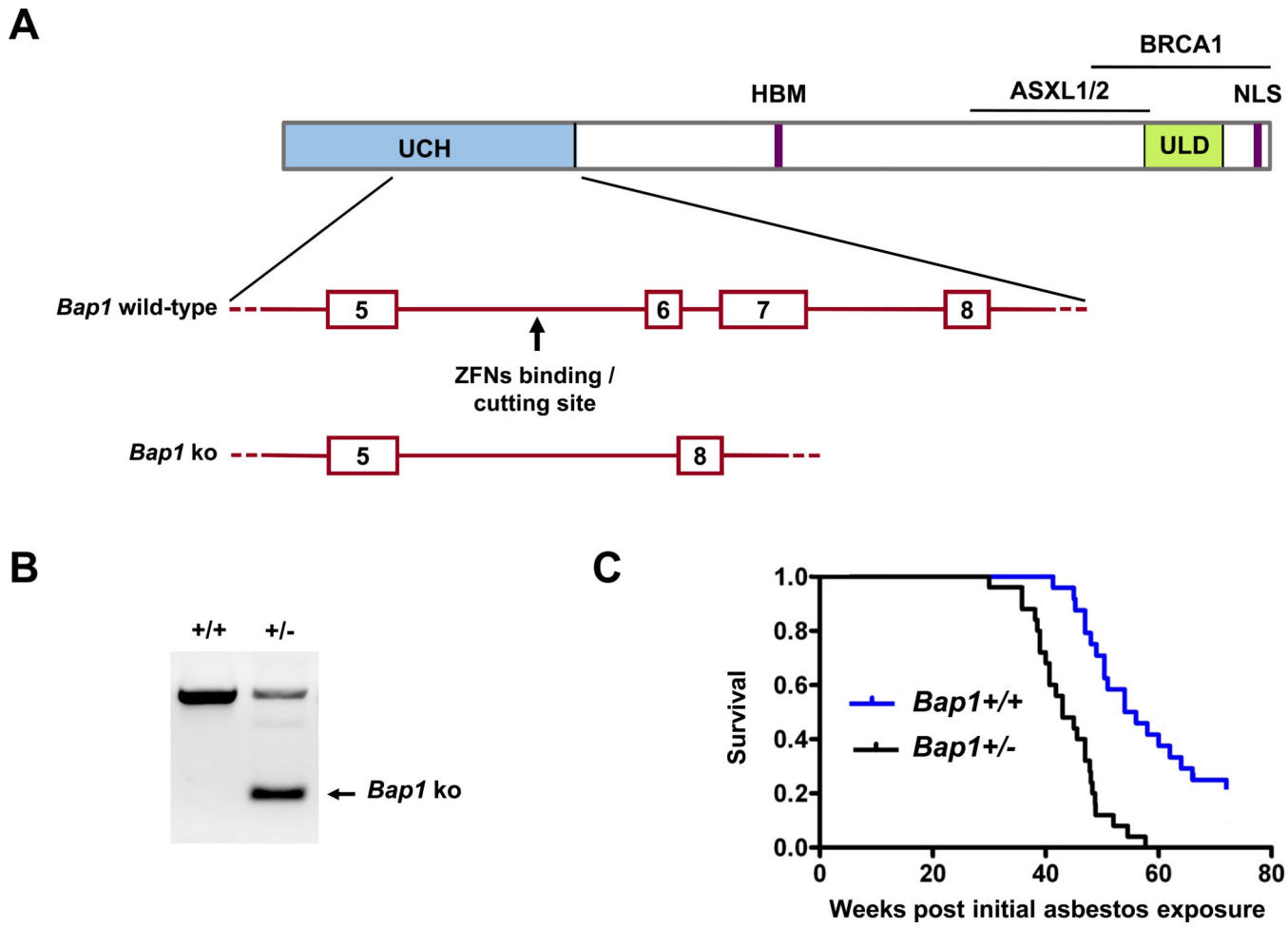

Figure 1.

Targeting of *Bap1* locus and induction of asbestos-induced MMs in *Bap1*$^{+/-}$ and WT mice. A, schematic diagram showing intronic cutting site (*arrow*) of ZFNs targeting *Bap1*, which resulted in loss of exons (boxes) 6 and 7 in *Bap1* knockout allele. Targeted region of *Bap1* locus corresponds to a portion of the UCH domain of BAP1 protein shown at the top. Abbreviations: ASXL1/2, additional sex combs like proteins 1 and 2 interaction domain; BRCA1, BRCA1 interaction domain; HBM, HCF1-binding motif; NLS, nuclear localization signal; UCH, ubiquitin C-terminal hydrolase; ULD, UCH37-like domain. B, genotyping of WT (+/+) and heterozygous (+/−)*Bap1* mice. Size of WT allele is 634 bp, and size of mutant allele (*arrow*) is 158 bp. C, Kaplan-Meier survival curves showing increased susceptibility to MM and shorter survival in asbestos-treated *Bap1*$^{+/-}$ mice than in asbestos-treated WT littermates. Survival differences were highly significant ($p < 0.0001$).

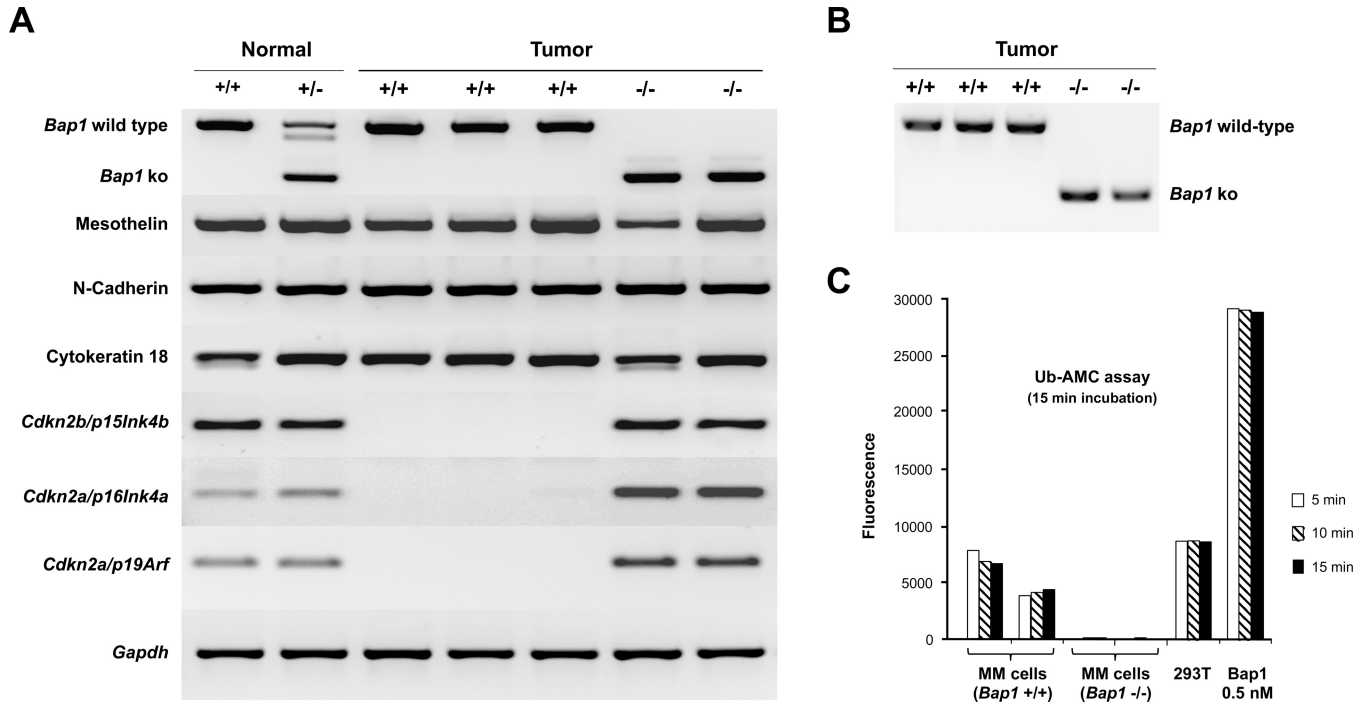

Figure 2.

Molecular analysis of asbestos-induced MMs in *Bap1*$^{+/-}$ and WT mice. A, RT-PCR analysis of expression of *Bap1*, various mesothelial markers, as well as *p16(Ink4a)*, *p19(Arf)*, and *p15(Ink4b)* in normal mesothelial cells and MM cells derived from asbestos-induced tumors from *Bap1*$^{+/-}$ and WT mice. Normal (+/+), normal mesothelial cells isolated from untreated WT mice. Normal (+/−), normal mesothelial cells isolated from untreated *Bap1*$^{+/-}$ mice. Tumor (+/+), MM cells derived from asbestos-exposed WT mice, retaining both alleles of *Bap1* and expressing wild-type Bap1. Tumor (−/−), MM cells derived from asbestos-exposed *Bap1*$^{+/-}$ mice, showing loss of expression of wild-type *Bap1*. B, PCR analysis of genomic DNA from *Bap1*(+/+) and (−/−) MM cells derived from WT and *Bap1*$^{+/-}$ mice, respectively. Note loss of WT allele in tumor cells from *Bap1*$^{+/-}$ mice. C, Ub-AMC assay demonstrating activity of Bap1 in MM cells from WT mice but not in MM cells from *Bap1*$^{+/-}$ mice.

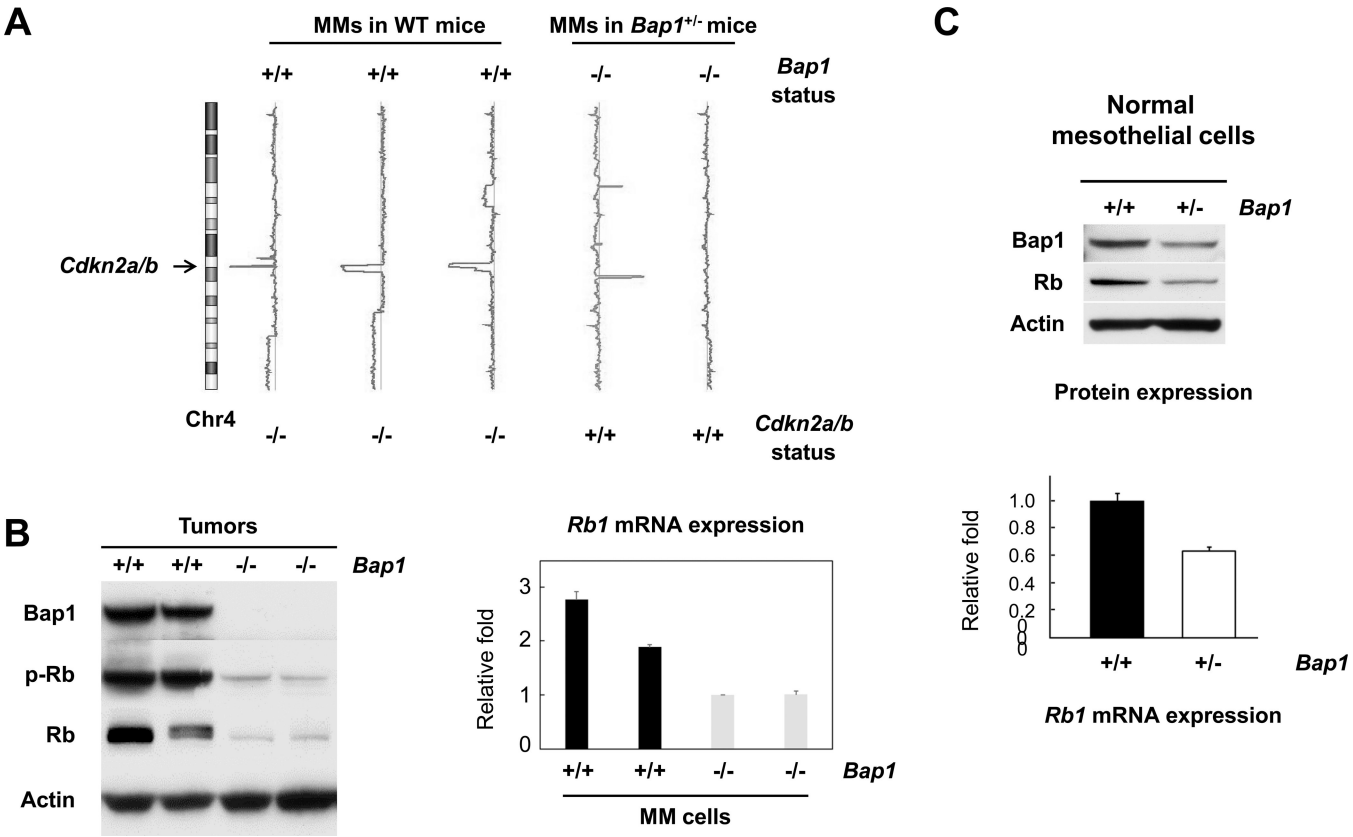

Figure 3.

Bap1-null MM cells derived from asbestos-induced tumors of *Bap1*$^{+/-}$ mice and normal mesothelial cells from *Bap1*$^{+/-}$ mice exhibit inactivation of Rb through a mechanism independent of *p16(Ink4a)* loss. A, aCGH profile of chromosome 4 (Chr4) showing homozygous loss of *Cdkn2a/Cdkn2b* loci at chromosome location 4qC4–qD1 in MM cells from WT mice, but not in MM cells from *Bap1*$^{+/-}$ mice. Note inverse correlation between *Bap1* loss and *Cdkn2a/b* loss in MM cells from WT mice and *Bap1*$^{+/-}$ mice. B, immunoblot analysis showing expression of Bap1, phospho-Rb and total Rb in MM cells (*left panel*). (+/+), tumor cells from asbestos-treated WT mice; (−/−), tumor cells from asbestos-treated *Bap1*$^{+/-}$ mice. Quantitative RT-PCR analysis of *Rb1* mRNA expression in *Bap1* (+/+) and (−/−) MM cells from WT and *Bap1*$^{+/-}$ mice, respectively, showing down regulation of *Rb1* at the transcriptional level in *Bap1*-null cells (*right panel*). C, Immunoblot analysis (*top panel*) and quantitative RT-PCR analysis (*bottom panel*) depicting down regulated expression of Rb protein and mRNA expression, respectively, in *Bap1*-haploinsufficient normal mesothelial cells from *Bap1*$^{+/-}$ mice compared to that in cells from WT mice.

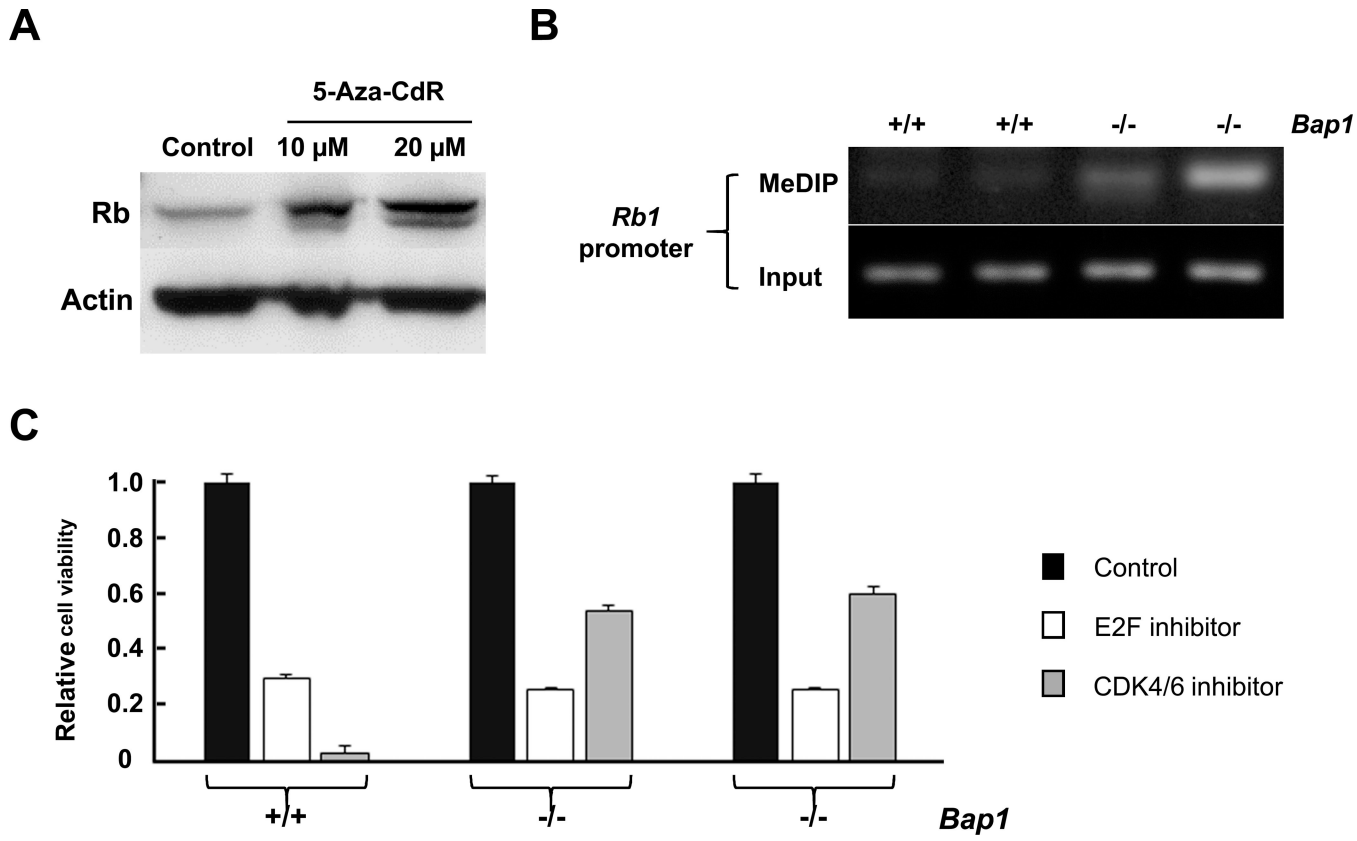

Figure 4.

Decreased expression of Rb results from aberrant epigenetic modification of the*Rb1* gene in MM cells from *Bap1*$^{+/-}$ mice, and Rb inactivation contributes to the malignant phenotype of these MM cells. A, total Rb expression in *Bap1*-null MM cells treated with 0 (control), 10 μM, and 20 μM of5-Aza-CdRfor 72 h. B, methylation analysis of *Rb1* promoter in *Bap1* (+/+) and *Bap1* (−/−) MM cells from WT and *Bap*$^{+/-}$ mice, respectively, by MeDIP assay followed by semi-quantitative PCR. Note that genomic DNA samples subjected to MeDIP show increased methylation of *Rb1* promoter in *Bap1*(−/−) MM cells compared to that of *Bap1*(+/+)cells. Input controls depict equivalent amounts of *Rb1* promoter DNA in all samples. C, treatment of MM cells with E2f inhibitor HLM006474(20 μM)or Cdk4/6 dual inhibitor LY2835219 (5 μM)and analyzed by MTS assay after incubation at 37°C for 72 h. Note that MM cells from both WT and *Bap1*$^{+/-}$ mice were sensitive to the E2f inhibitor, whereas tumor cells from WT animals, which lacked expression of p16(Ink4a), were much more sensitive to a Cdk4/6 inhibitor than *Bap1*-null cells that retained expression of p16(Ink4a).